Current Integrative Engineering
Volume 2, Issue 1, 42-59, *ISSN: 2995-6307*
DOI: 10.59762/cie570390542120240205133744

Characterization Of Resonant Coupled Inductor In A Wireless Power Transfer System

Alan P. Nebrida
Faculty, Department of Electrical Engineering, Nueva Vizcaya State University, Bambang, Nueva Vizcaya, 3702 Philippines

Abstract
Wireless power transfer (WPT) has garnered significant interest as a potentially transformative technology in the energy sector, as it presents a novel approach to powering and charging devices. The functionality of this technology is predicated upon the utilization of electromagnetic coupling to facilitate the wireless transmission of energy between two entities. Despite the considerable potential, wireless power transfer (WPT) faces significant obstacles that restrict its practical feasibility. One notable challenge that arises is the decrease in power transfer efficiency as the distance between the transmitter and receiver increases. Moreover, the Wireless Power Transfer (WPT) technology is further limited by its reliance on accurate alignment between the transmitting source and the receiving device, thereby posing challenges for its practical implementation. The issues present substantial obstacles to the widespread commercialization of wireless power transfer (WPT). This study seeks to improve the efficacy of power transfer by optimizing the resonance frequency of the power transfer in response to the challenges. By systematically manipulating various parameters, including coil dimensions, input voltage levels, and operational frequency, a novel approach is proposed to enhance the efficiency of power transfer. The study additionally offers valuable insights regarding the correlation between the distance separating the coils and the efficiency of power transfer. The findings of this study offer a thorough empirical analysis and are supported by a strong theoretical framework, resulting in a substantial coefficient of determination (R^2 = 0.937118). This finding suggests that the linear regression model under consideration could account for approximately 93.7118 percent of the variability observed in the distance. The findings of this study establish a pathway towards enhanced and feasible wireless power technology, thereby establishing a robust basis for the prospective commercial implementation of wireless power transfer (WPT) systems.

Keywords: Wireless Power Transfer, Coupled Magnetic Resonance, Resonance Frequency, Inductive Coupling,

Introduction

In today's world, there has been a notable surge in the production and enhancement of portable electronic devices, including mobile phones, laptops, and various other electronics and communication devices. Irrespective of their wireless communication capabilities, these devices necessitate periodic charging, typically accomplished by connecting them to a power source via a wall outlet. This phenomenon amplifies the pursuit of novel methodologies aimed at enabling wireless power transmission to enhance the portability and mobility of such devices for end-users. Wireless energy transfer, also known as Wireless Power Transfer (WPT), refers to the transmission of electrical energy from a power source to an electrical load without the use of physical wires for interconnection. Various physiological techniques, such as laser technology, the piezoelectric principle, radio waves, microwaves, inductive coupling, and strong electromagnetic resonance, have been employed thus far for the purpose of wireless energy transfer. The utilization of a

Alan P. Nebrida
Faculty, Department of Electrical Engineering, Nueva Vizcaya State University, Bambang, Nueva Vizcaya, 3702 Philippines
ap_nebrida@nvsu.edu.ph

Received: Nov-09-2023 Revised: Dec-26-2023 Accepted: Feb-13-2024

magnetic field for the transmission of substantial quantities of power ultimately gives rise to dissatisfaction and potential health hazards for individuals. The efficacy of the technique is notable; however, it is accompanied by a limitation due to its reliance on an unobstructed line of sight and the potential for harm to living organisms stemming from its underlying mechanism. Wireless energy transfer through the utilization of electromagnetic resonance phenomena has emerged as a viable option, particularly for short distances, owing to its notable attributes such as high-power transfer efficiency and the absence of adverse impacts on human health. According to the study conducted by Karalis et al. (2008), The technologies of wireless power transfer (WPT), electromagnetic induction, and microwave power transfer have gained significant recognition in academic and scientific fields. Nevertheless, the concept of electromagnetic resonance couplings has only emerged in recent times. The wireless power transfer technology necessitates the incorporation of three primary components: substantial air gaps, optimal efficiency, and a significant power output. Electromagnetic resonance coupling represents the sole technological approach that addresses the three elements. The primary aim of this study is to provide a comprehensive characterization of resonant coupled inductors utilized in wireless power transfer systems. The primary objectives of this study are as follows: (1) To devise a wireless power transfer system; (2) To construct a model of the wireless power transfer system and execute simulations; (3) To ascertain the maximum distance over which the model can transmit power effectively, considering various orientations of the power transmitter; (4) To compare the outcomes of the simulations with empirically measured values; and (5) To formulate a systematic approach for analyzing data and establishing a methodology for characterizing wireless power transmission systems. In contemporary times, engineers and designers engaged in the advancement of household devices are required to offer consumers an enhanced degree of convenience and adaptability. The investigation focused on a Wireless Power Transfer (WPT) system as a potential solution for addressing the inconvenience associated with the utilization of a power cable. The utilization of wireless transmission proves advantageous in situations where the installation of interconnecting wires is impractical, poses risks, or is unfeasible. The attainment of wireless power transfer will enhance the portability and mobility of electronic devices by significantly improving the convenience of the charging process and eliminating the need for cord insertion into a socket. Furthermore, in the context of wireless charging, the safety of the charging process is enhanced by mitigating the risk of electric shock resulting from the deterioration of an aged cord. The present study employs resonant inductive coupling as a means of wireless power transfer. The research study employs a low power supply for the purpose of power transmission. The study's focus is confined to the development of a simplified wireless power transfer (WPT) system utilizing a resonant-coupled inductor configuration. This study encompasses several components, namely the matching sections, the derivation of the relationship between the coupling coefficient and distance, and the examination of various parameters such as the quality factor, coupling coefficients, mutual inductance, and resonance frequency of the resonators. To facilitate the discernment of the system's operational status, the investigator employs a 12V, 5W CYD LED bulb as the designated load. This study will not encompass alternative approaches for enhancing the efficacy of wireless power.

Methodology

The present research investigation employed a systematic methodology in the development, creation, and evaluation of the suggested system. The methodology is visually depicted in Figure 1, which is appropriately labeled as the Methodology Flow Chart. The chart presented herein offers a systematic representation of the sequential actions undertaken throughout the duration of this research endeavor. The collection and analysis of data constitute the preliminary stage of the research methodology. This stage encompasses the establishment of the specifications for both the hardware and software elements, facilitating the formulation of the project's design. The design phase of the study encompasses meticulous deliberation regarding the hardware and

Current Integrative Engineering
Volume 2, Issue 1, 42-59, *ISSN: 2995-6307*
DOI: 10.59762/cie5703905421202402051337 44

software components of the system. The process encompasses the establishment of a conceptual framework and the identification of the requisite materials for the hardware implementation. This phase encompasses the determination of the algorithm, program flow, and software type necessary for the implementation of the software. After the completion of the design phase, the project assembly was conducted, followed by the execution of testing, and debugging procedures. During this phase, essential modifications were implemented to guarantee the system's optimal performance. Subsequently, the integration of both hardware and software components occurred, thereby facilitating the commencement of thorough testing procedures. The subsequent phase entailed the execution of a sequence of experiments with a specific emphasis on the variables under investigation in the study. These variables include the distances between the transmitting and receiving coils, resonant frequency, voltage gain, and system efficiency.

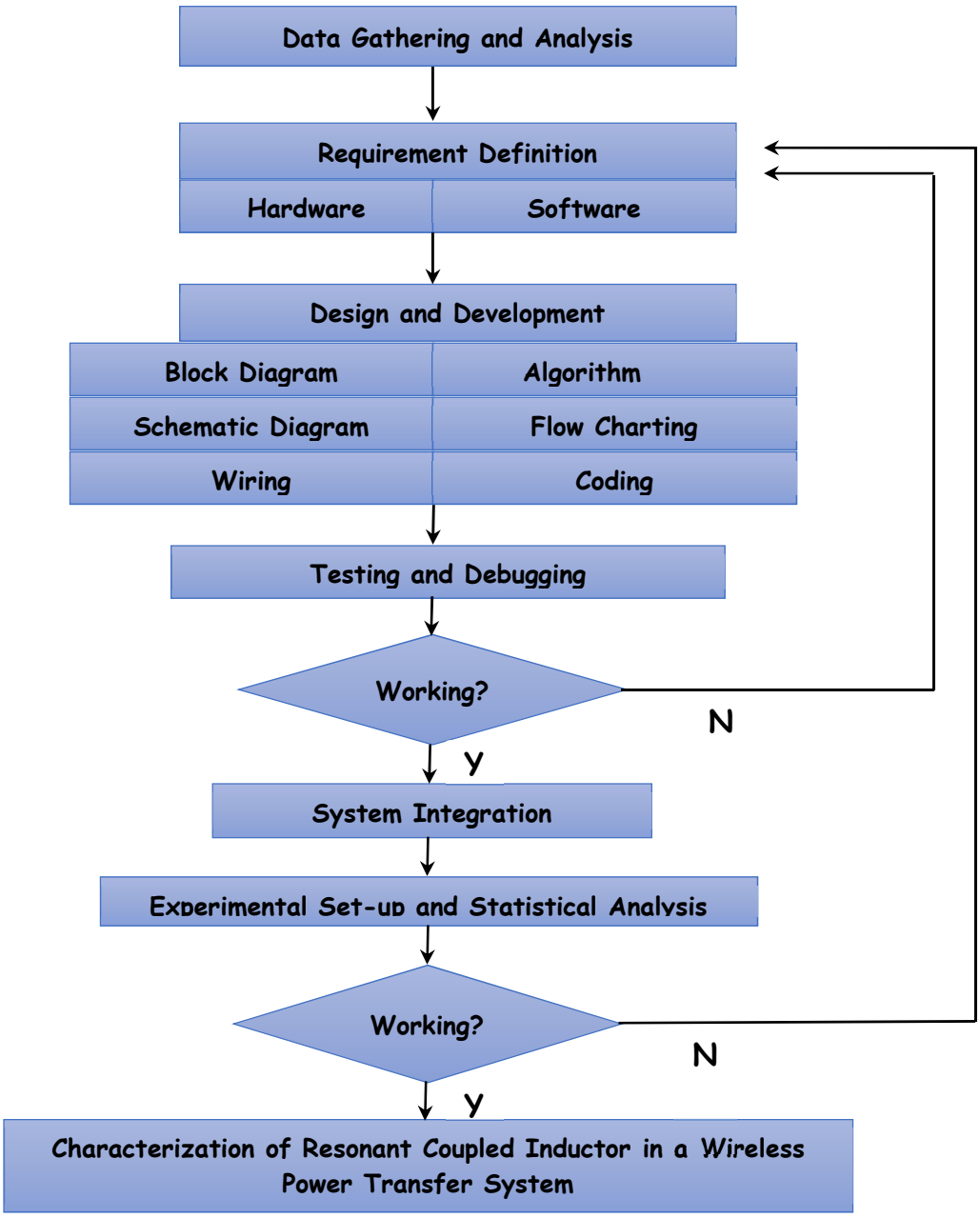

Figure 1.
Methodology Flow Chart

The determination of the parameters of the Resonant Coupled Inductor in the Wireless Power Transfer System was predominantly derived from the outcomes of these experimental investigations. Comprehensive analyses of the findings are expounded upon in subsequent sections of this scholarly article.

Conceptualization/Development of System Design

System Block Diagram

The system, as depicted in Figure 2, is structured into four main sections, all of which are essential for the system's overall functioning. The initial component, known as the Power Amplifier, assumes a pivotal role within the system. The device is accountable for amplifying the power of the input signal. The radio frequency signal is amplified to a suitable level for transmission. The ability to adjust the output power allows for precise control over the desired signal strength, thereby playing a crucial role in optimizing the efficiency of wireless power transmission. The subsequent section encompasses the Transmitting Loops, which serve as the primary antennas within the system. The primary purpose of power amplifiers is to transmit amplified signals to the surrounding environment. The amplified electrical signals are converted into electromagnetic waves that have the ability to propagate through space by the transmitting loops. The devices are intricately engineered to function at the resonant frequency of the system, thereby enabling efficient energy transfer. The third section comprises the Receiving Loops, which function as the receiving antennas of the system. These devices have been designed to effectively capture electromagnetic waves emitted by transmitting loops and subsequently convert them into electrical signals. Like the transmitting loops, these devices are also specifically engineered to function at the resonant frequency of the system, thereby optimizing the absorption of energy from the electromagnetic waves being transmitted. The last component of the system is the Voltage Rectifier, which is responsible for the con-

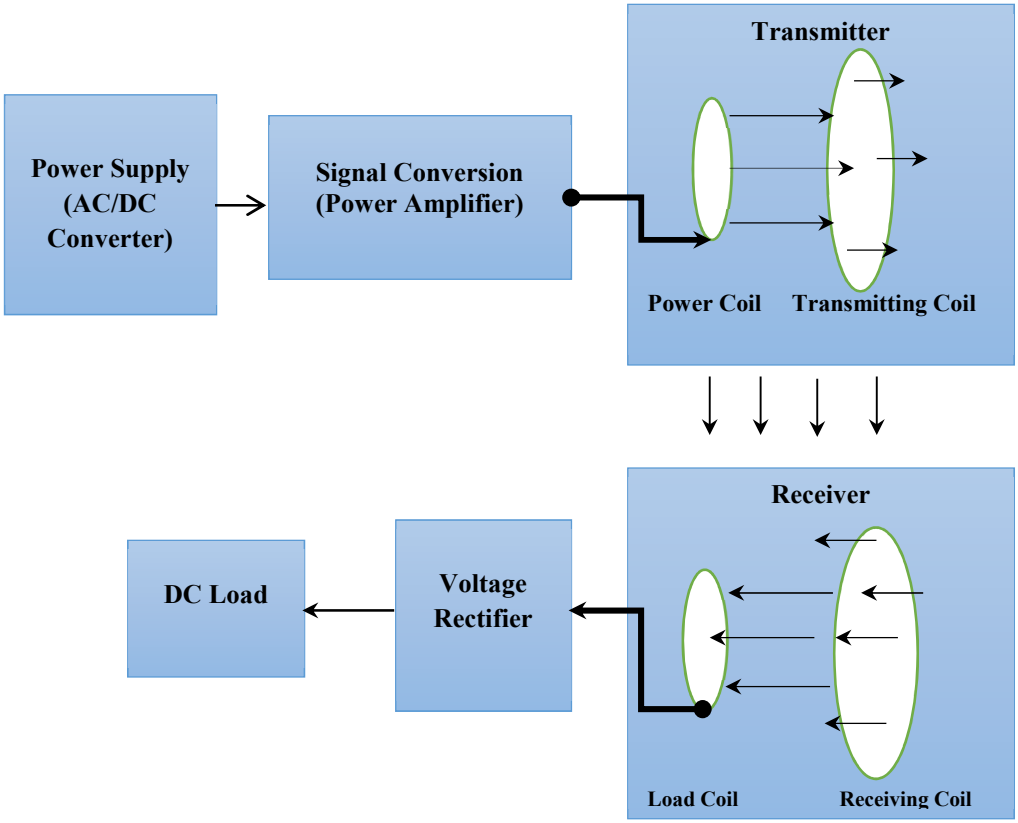

Figure 2.
The Block Diagram of the System

Current Integrative Engineering
Volume 2, Issue 1, 42-59, *ISSN: 2995-6307*
DOI: 10.59762/cie5703905421202402051337 44

version of the alternating current (AC) produced by the receiving loops into direct current (DC). Since a multitude of electronic devices require direct current (DC) for their functioning, the significance of this component becomes paramount in the context of implementing wireless power transmission in real-world scenarios.

Every component of the system has been meticulously crafted to align with the precise objectives of the study. Any alteration made to each individual section has the potential to directly impact the overall performance of the system, encompassing both efficiency and power transfer range. Hence, meticulous consideration is devoted to the design and implementation of each section, to guarantee that the overall system achieves optimal performance in accordance with the research objectives.

Amplifier

The amplifier plays a crucial role in ensuring the effective functioning of the wireless power transfer system, as outlined in the description. The primary purpose of this device is to amplify the input oscillating signal to produce a robust magnetic flux that can effectively induce the highest possible voltage in the receiving loop. The utilization of this function is imperative for the effective and streamlined functioning of wireless power transfer systems. The amplifier's design is specifically engineered to facilitate the integration of a feedback loop originating from the transmitting antenna or loop. The distinctive arrangement of components enables the redirection of the antenna's resonant frequency towards the amplifier, resulting in a reliable and robust amplification of the signal. The utilization of this feedback mechanism serves as the foundation for the overall optimization and efficacy of the wireless power transfer system. The utilization of Multisim software simulations played a crucial role in both the design and testing phases of the amplifier. Although it is recognized that the Multisim library did not include the precise components employed in physical bench testing, appropriate generic components were employed to ensure the fidelity of the simulations. In this context, Multisim has demonstrated its significant utility as a valuable tool for the prediction and comprehension of circuit behaviors, particularly with respect to resonance and amplification parameters. The schematic diagram of the amplifier is depicted in Figure 3, which represents the simulated circuit. The tank circuit, denoted by the components C1 and L3, functions as a reflection of the

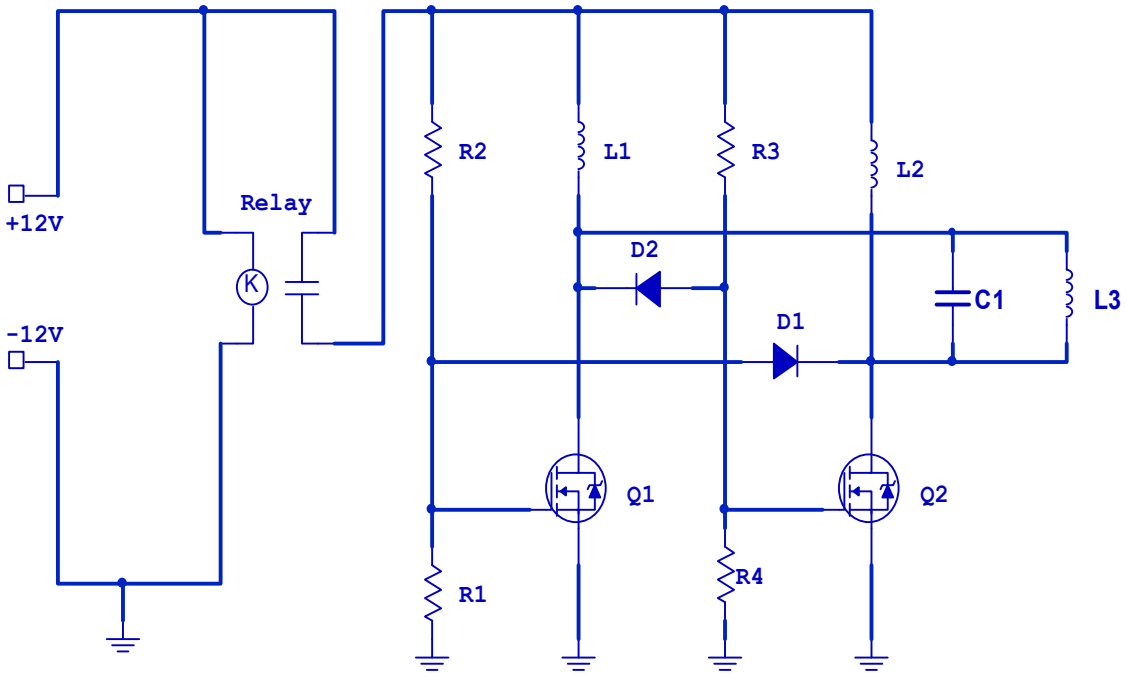

Figure 3.
Schematic Diagram of Amplifier

antenna load, and its parameters are deliberately selected to achieve resonance at a frequency of 580kHz. The incorporation of this design element serves to optimize the transfer of resonant energy, which is a primary objective of the present study.

Figure 4 offers significant insights into the operational characteristics of the amplifier as observed in the simulation. The tank circuit effectively generated oscillation, which is a vital component of the system's functioning. The oscillation was subsequently amplified via the MOSFET, thereby confirming the theoretical functionality of the amplifier. Although the simulation had certain limitations arising from the utilization of generic components, it effectively demonstrated the funda-

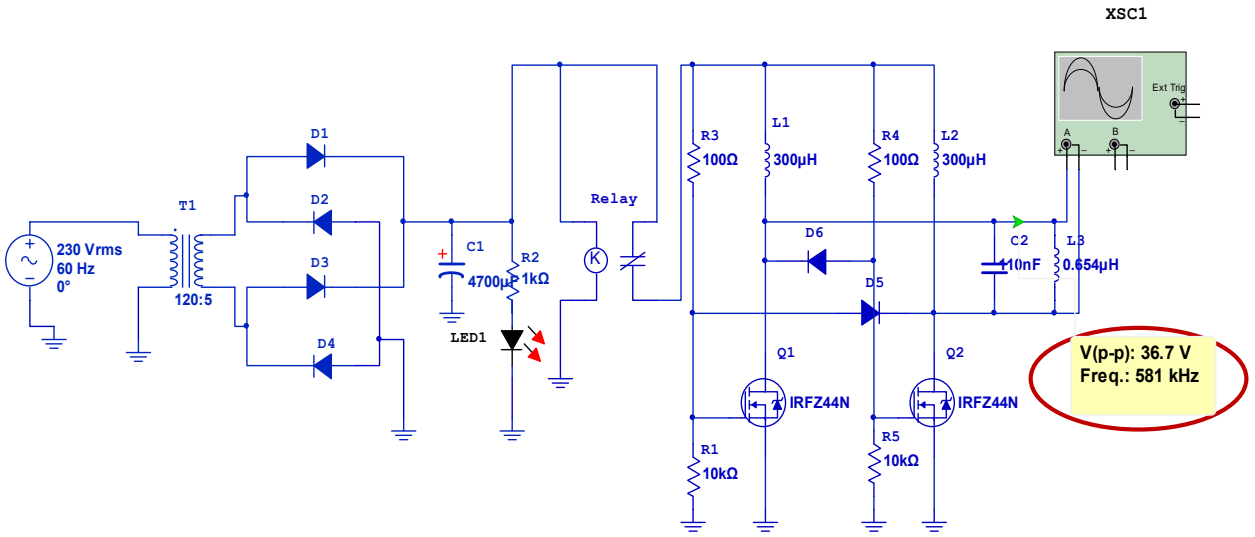

(a)

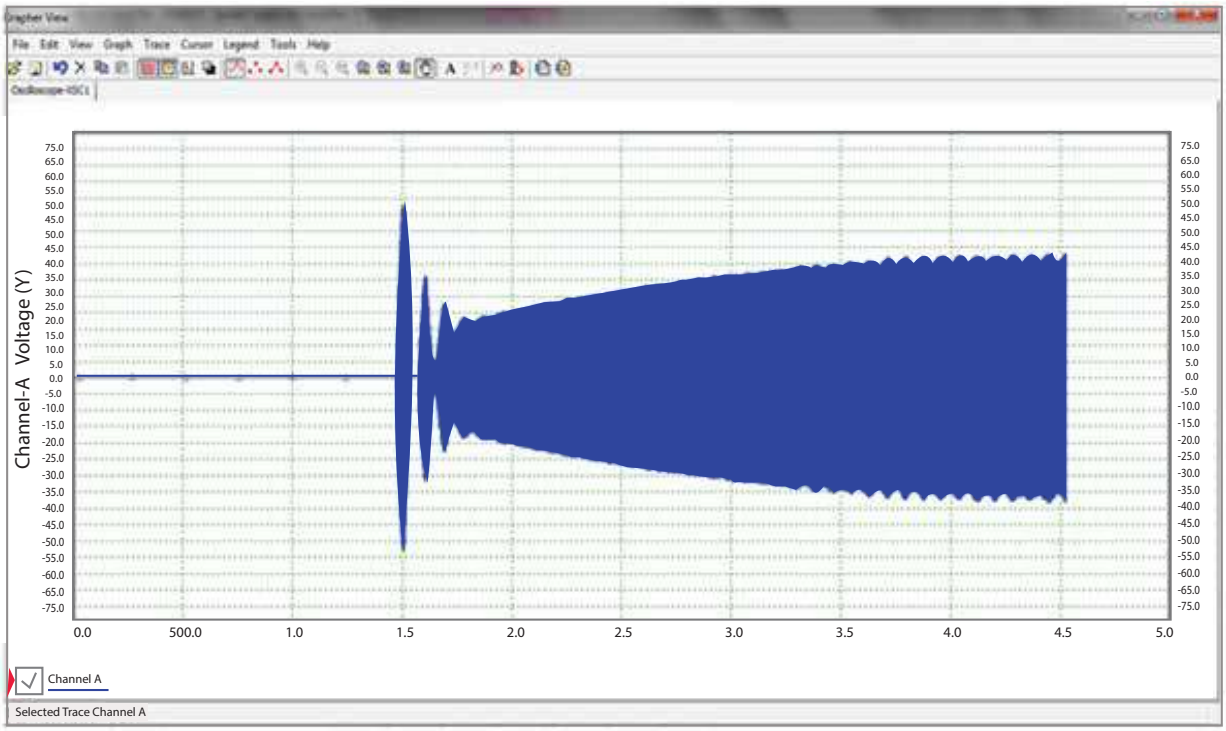

(b)

Figure 4.
Amplifier output in Multisim using (a) Measurement Probe, (b) Oscilloscope

Current Integrative Engineering
Volume 2, Issue 1, 42-59, *ISSN: 2995-6307*
DOI: 10.59762/cie5703905421202402051337 44

mental operational principles of the amplifier. The obtained simulation results, as depicted in Figure 4(a), demonstrate that the operating frequency closely approximates the desired value of 580 kHz. This observation suggests that the amplifier is effectively performing its intended function. The amplifier successfully operated, as evidenced by the achievement of an output voltage of approximately 36.7 volts peak-to-peak.

Transmitter and Receiver Loops

The coupling circuit, consisting of the transmitter and receiver loops, constitutes the fundamental component of the wireless power transfer system. The coupling circuit is the location where the effective transmission of wireless power takes place, and the distances between the transmitter and receiver significantly influence its efficiency. The design of the transmitter and receiver loops allows for a variable separation along their respective axes. This functionality facilitates the examination and measurement of the impact of the distance of separation on the overall effectiveness of the system. Measurements were performed on a direct current (DC) load at various distances, and the outcomes are illustrated in Figure 3.13. The findings of this study offer significant insights into the influence of distance on the efficiency of power transfer within the system, thus emphasizing the significance of separation distance in the optimization of the design and performance of wireless power transfer systems.

Voltage Rectifier

The voltage rectifier is an essential element within the system. The device is tasked with the conversion of the received alternating current (AC) voltage from the load coil into a direct current (DC) voltage, thereby enabling its use for powering a DC load. The Full Wave Bridge Rectifier has been selected as the preferred rectifying circuit for this application due to its capability to produce an output voltage that is exclusively direct current (DC) or possesses a predetermined DC component. The rectifier in question employs a closed loop "bridge" configuration consisting of four interconnected rectifying diodes to achieve the intended output. To mitigate the ripple present in the full-wave rectifier output, a smoothing capacitor is connected to the bridge circuit. The purpose of this arrangement is to convert the rippled output of the rectifier, which is a full-wave waveform, into a steady direct current (DC) voltage. This ensures a consistent and uninterrupted DC voltage supply for the load. The selection of diodes for the rectifier holds significant importance in the design process, particularly when considering the rectification of high-frequency signals. The selection of fast signal diodes, specifically the 31DF4 type, for this system, was based on their ability to efficiently rectify alternating current (AC) signals at frequencies in the megahertz range.

Circuit Model and Transfer System

The resonator system, illustrated in Figure 5, can be understood by considering the lumped circuit components: L (inductor), C (capacitor), and R (resistor). The provided diagram depicts a circuit configuration that is well-suited for both manual analysis and SPICE simulations.

Figure 5 depicts a circuit diagram that is visually enhanced with illustrations. The diagram showcases the presence of four resonant circuits, which are interconnected through magnetic coupling coefficients denoted as k12, k23, and k34. The power loop is energized by a source possessing a finite output impedance, denoted as RS, commencing from the left. The power loop can be represented by a single-turn inductor, denoted as L1, which is accompanied by a corresponding resistance, denoted as R1. The inclusion of capacitor C1 serves to establish resonance at the intended frequency within the power loop. The transmitter loop, denoted as Tx, consists of two components: the parasitic resistance R2 and a single-turn air core inductor L2. The self-capacitance, denoted as C2, is determined by the geometry of the Tx loop. The inductors L1 and L2 are interconnected with a coupling coefficient k12, and the receive side is defined similarly. The interconnection between the transmitter and receiver loops is established through the coupling coefficient, denoted as k23. In a conventional implementation, the drive loop and the Tx coil would be combined into a unified entity, thereby resolving the issue of k12. Similarly, the value of k34 would also remain constant. As a result, k23 would represent the sole uncontrolled variable, subject to variation depending on the distances separating the transmitting and

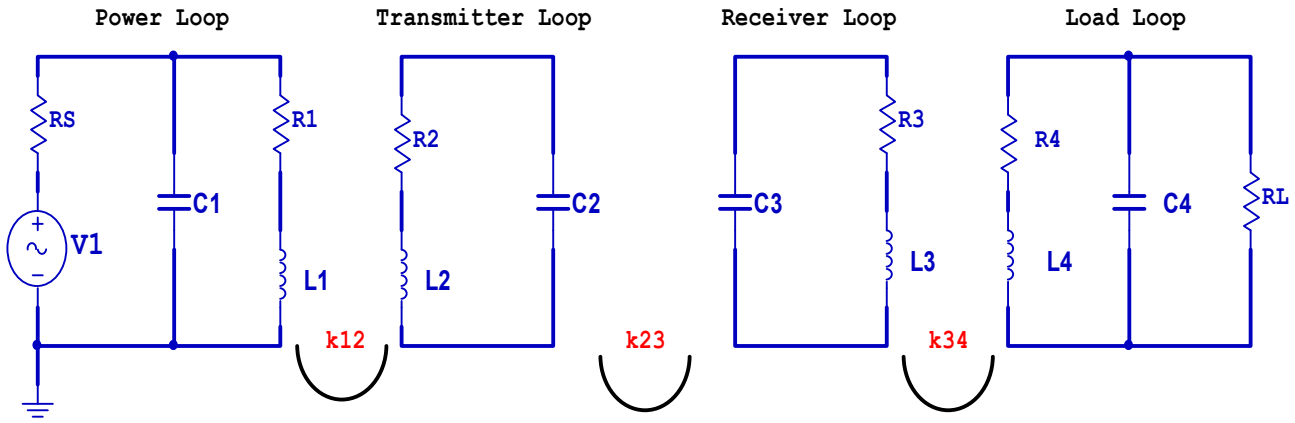

Figure 5.
Equivalent Circuit Model of the System

receiving entities. The parallel resonators in the model represent each of the four antenna elements, which are interconnected by mutual inductances and coupling coefficients.

One effective approach for examining the transfer characteristics of a resonator system with magnetic coupling is to utilize the circuit model as a point of reference. To maintain simplicity in the analysis, the cross-coupling terms k12 and k34 are neglected. The circuit model provides a straightforward method for systematically examining the characteristics of the system. The utilization of Kirchhoff's Voltage Law (KVL) enables the representation of the connection between the current passing through each coil and the voltage applied to the power coil, as illustrated in equation 1. This is achieved by determining the currents in each resonant circuit, as illustrated in Figure 5. The coupling coefficient is defined by Equation 2.

$$\begin{bmatrix} V_s \\ 0 \\ 0 \\ 0 \end{bmatrix} = \begin{bmatrix} Z_1 & j\omega M_{12} & 0 & 0 \\ j\omega M_{12} & Z_2 & -j\omega M_{23} & 0 \\ 0 & -j\omega M_{23} & Z_3 & j\omega M_{34} \\ 0 & 0 & j\omega M_{34} & Z_4 \end{bmatrix} \begin{bmatrix} i_1 \\ i_2 \\ i_3 \\ i_4 \end{bmatrix} \quad (1)$$

$$k_{xy} = \frac{M_{xy}}{\sqrt{L_x L_y}}, \qquad 0 \leq k_{xy} \leq 1 \quad (2)$$

The symbol "M_{xy}" is used to represent the concept of mutual inductance between two coils, denoted as "x" and "y." Additionally, the symbols Z_1, Z_2, Z_3, and Z_4 are employed to represent the loop impedances of these four coils. The impedances are designated correspondingly.

$$Z_1 = R_s + \frac{R_1 + j\omega L_1}{\omega^2 L_1 - j\omega C_1 R_1 + 1} \quad (3)$$

$$Z_2 = R_2 + j\left(\omega L_2 - \frac{1}{\omega C_2}\right) \quad (4)$$

$$Z_3 = R_3 + j\left(\omega L_3 - \frac{1}{\omega C_3}\right) \quad (5)$$

$$Z_4 = R_L + \frac{R_4 + j\omega L_4}{\omega^2 L_4 - j\omega C_4 R_4 + 1} \quad (6)$$

The calculation of the current ($_{i4}$) in the load coil resonant circuit is determined by utilizing the matrix in equation 1 through the application of the substitution method.

$$i_4 = -\frac{j\omega^3 M_{12} M_{23} M_{34} V_s}{Z_1 Z_2 Z_3 Z_4 + \omega^2 M_{12}^2 Z_3 Z_4 + \omega^2 M_{23}^2 Z_1 Z_4 + \omega^2 M_{34}^2 Z_1 Z_2 + \omega^4 M_{12}^2 M_{34}^2} \quad (7)$$

The voltage across the load, denoted as V_L, can be expressed as $-i_4 R_L$, where i4 represents the current flowing through the load and R_L represents the load resistance. Additionally, a voltage-to-voltage relationship, denoted as V_L/V_s, exists between the source voltage (V_s) and the load voltage (V_L). The system model bears resemblance to a two-port network. The S-parameter is a suitable metric for evaluating the efficiency of this system. The vector S21 quantifies the relationship between the signals leaving the output ports and the signals entering the input ports. The efficiency of power transfer is contingent upon the power gain, which is determined by the parameter $|S_{21}|^2$, representing the squared magnitude

Current Integrative Engineering
Volume 2, Issue 1, 42-59, *ISSN: 2995-6307*
DOI: 10.59762/cie5703905421202402051337 44

of S_{21}. The calculation of the S_{21} parameter is based on the work of Sample et al. (2011), as referenced in the studies conducted by Fletcher and Rossing (1998) and Mongia (2007).

$$\boldsymbol{S_{21} = 2\frac{V_L}{V_S}\left(\frac{R_s}{R_L}\right)^{1/2}} \quad (8)$$

Therefore, by incorporating the equation $M_{xy}=k_{xy}\sqrt{(L_x L_y)}$ derived from equation 2, the S_{21} parameter can be expressed as

$$\boldsymbol{S_{21} = \frac{j2\omega^3 k_{12}k_{23}k_{34}L_2L_3\sqrt{L_1L_4R_sR_L}}{Z_1Z_2Z_3Z_4 + {k_{12}}^2L_1L_2Z_3Z_4\omega^2 + {k_{23}}^2L_2L_3Z_1Z_4\omega^2 + {k_{34}}^2L_3L_4Z_1Z_2\omega^2 + {k_{12}}^2{k_{34}}^2L_1L_2Z_3Z_4\omega^2}} \quad (9)$$

The utilization of equation 9 for the analysis of the system's performance proves to be advantageous. The efficiency of the system is determined by the parameter known as the magnitude of S21. This parameter can be expressed as a function of two variables, namely k23 and frequency. The values of all circuit parameters can be found in Table 1. The coupling coefficient k23, as previously mentioned, is the parameter that undergoes changes in response to alterations in circumstances. The presence of a variable distance can result in variations in k23. Moreover, alterations in the orientation or misalignment of the transmitting and receiving resonators have an impact on the coefficient. The mutual inductance between the coils exhibits a negative correlation with distance, implying that an increase in distance will result in an increase in the value of k23. The k23 undergoes a modification when there is a variation in orientation or misalignment. The graphical representation in Figure 6 illustrates the interconnections among S21, k23, and frequency. Based on the data presented in the figure, it can be observed that for scenarios where k23 is small, such as instances involving significant separation between the transmitter and receiver or a combination of misalignment and orientation deviation, the efficiency, as indicated by the magnitude of S21, exhibits a maximum value at the self-resonant frequency of approximately 580kHz. Consequently, the resonant frequency undergoes variation in response to alterations in k_{23}. A thorough analysis of the relationship between the magnitude of S21 and the variable k23 yields valuable insights. The magnitude of S21 exhibits a diminished value when the coefficient k23 assumes a significantly small value, a circumstance that arises when the distance between the transmitter and receiver is excessively large. The magnitude of |S21| exhibits an increase as the separation between the resonators decreases, which is attributed to an augmentation in the value of k23. However, increasing the value of k23 does not necessarily lead to a higher magnitude of |S21| once the threshold level of |S21| is attained. Furthermore, a notable issue arises regarding frequency splitting, which substantially diminishes the efficiency of the apparatus. The location within the system at which the initial resonance frequency (593.383 kHz) deviates hold considerable influence. The superior performance of the system is evident through the relative positioning of the resonators. The efficiency is inadequately characterized when the distance exceeds the specified range. However, the efficiency remains high despite the detuning of the resonant frequency in two furrows. Optimal power transmission would be achieved if the frequency could be adjusted to the desired frequency.

Parameter	Value
$R_S,\ R_L$	50Ω
$L_1,\ L_4$	$0.654\mu H$
$C_1,\ C_4$	$110nF$
$R_1,\ R_4$	0.20Ω
$L_2,\ L_3$	$0.944\mu H$
$C_2,\ C_3$	$80nF$
$R_2,\ R_3$	0.20Ω
k_{23}	$0.001\ to\ 0.30$
f_o	$580\ kHz$
$frequency$	$100kHz\ to\ 1.5MHz$

Table 1.
Component Values in the Circuit model.

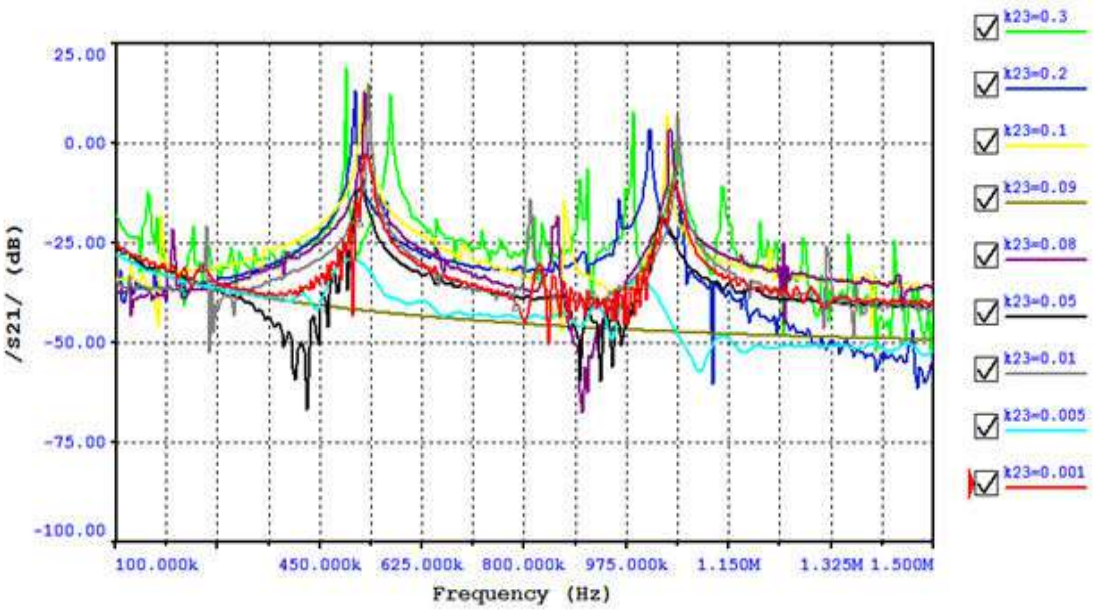

Figure 6.
$|S_{21}|$ as a Function of k_{23} and frequency

Experimental Results and Validation

Based on the previously proposed framework, the experimental apparatus has been constructed, and the investigation of energy transfer reveals a wide range of potential applications for this technology in the coming years. The structure of the inductive coupling between the source, transmitting resonator, receiving resonator, and load is illustrated in Figure 7. The source is denoted by the initial loop on the leftmost side (final loop on the rightmost side). The experimental setup employed to validate the theoretical model is depicted in Figure 7. The left-side transmitter comprises a compact drive loop positioned at the center of a larger loop resonator, with a separation distance of 0.7 cm. The diameter of the drive loop measures 30 cm, and a capacitor connected in parallel is employed to adjust the system's tuning to a frequency of 593.383 kHz. The transmit loop is of considerable size and possesses an outer diameter measuring 40 cm. The experimental determination of the resonant frequency was found to be 593.383 kHz. The receiver is constructed similarly and is positioned at the same distance as the transmitter. The constituent components of the structure consist of copper tubes with a diameter of 13 mm, which are reinforced by Plexiglas armatures. A notable obstacle encountered in the process of comparing the theoretical model with empirical data lies in the precise estimation of the lumped circuit parameters L, C, and R pertaining to the physical system. To achieve the objective, we employed established RF and microwave measurement methodologies that have been developed for the purpose of extracting key parameters from resonant structures, including resonant frequency, coupling coefficient, and unloaded Q factor. One of the benefits of this technology is its ability to facilitate energy transfer across a range of different objects. Various types of obstacles were strategically positioned between the transmitting and receiving loops to assess their capacity to penetrate objects. The experimental findings demonstrate that energy transfer remains feasible even when the recipient is protected under various circumstances. According to the findings, it has been observed that non-metallic objects, including walls, books, wooden products, organic glass panels, leather, and textiles, do not exert any influence on the transfer of power.

In Figure 7, the experimental apparatus for energy transfer is depicted the influence of metallic objects on the system is contingent upon various characteristics of the metal conductor. As previously discussed by Zhu et al. (2008),

Current Integrative Engineering
Volume 2, Issue 1, 42-59, *ISSN: 2995-6307*
DOI: 10.59762/cie5703905421202402051337 44

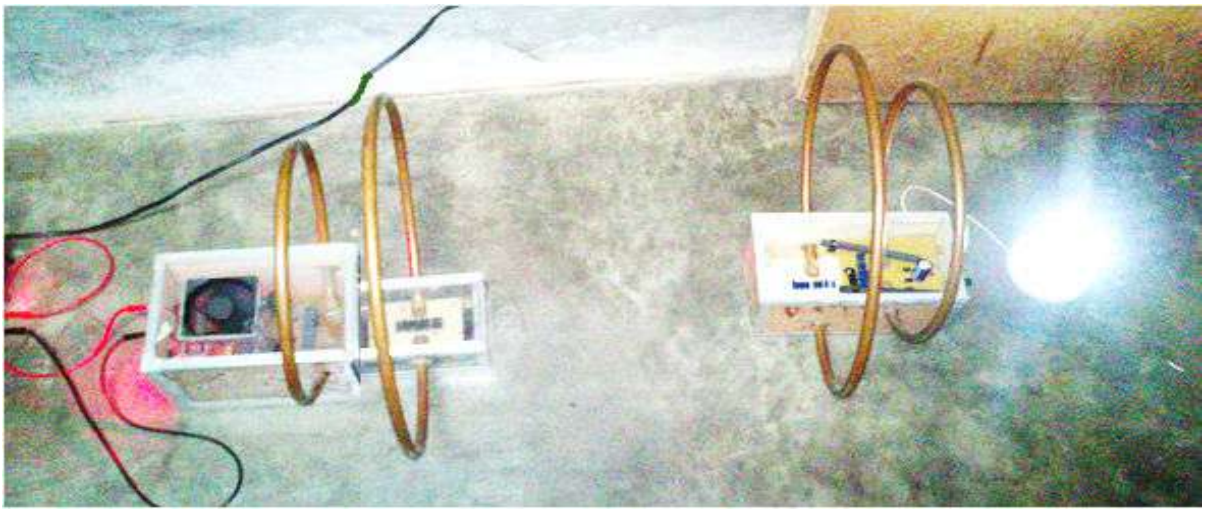

Figure 7.
The Energy Transfer Experimental Device

the impact would be minimal if the object is smaller than the diameter of the coil or if it is unable to generate a significant eddy current. If metallic objects that can generate larger eddy currents or forming a closed loop are near this system, the resulting impact will be more significant, potentially hindering the transfer of energy. Based upon the data collected on Table 2, the following graph shows voltage as a function of distance between the loop, the transmitter and receiver. Curves in figure 8 show the impact on the output voltage caused by different transfer di early fit, the data points were strongly correlated. To put it another way, the Power Transfer Efficiency rapidly declines as a function of distance outside the linked mode zone. This exemplifies the hypothesis that coupled mode resonance vanishes as the distance between the two antennas grows, allowing the antennas to operate in the near field as conventional transmitting and receiving antennas. Figure 9, shown below, illustrates the relationship between voltage gain and distance. It is seen that as the distance decreases, the voltage gain increases. Therefore,

Distance (cm)	Output Voltage (Volts)	Distance (cm)	Output Voltage (Volts)	Distance (cm)	Output Voltage (Volts)	Distance (cm)	Output Voltage (Volts)
0	10.83	30	8.09	60	2.73	90	0.603
5	10.15	35	7.04	65	2.07	95	0.469
10	9.79	40	6.29	70	1.57	100	0.345
15	9.68	45	5.43	75	1.212	105	0.246
20	9.45	50	4.83	80	0.975	110	0.006
25	9.24	55	3.58	85	0.742	115	0.007

Table 2.
Relationship between Receiver Output Voltage and Distance

tance. It is obvious that the longer is the distance between the two loops, the lower the output voltage of the receiving loop is. Since the coefficient of determination R^2 has a value close to 1 for the linan increased separation between the transmitting and receiving coils results in a decrease in the gain voltage. The graph reveals the presence of a finite separation between the two coils.

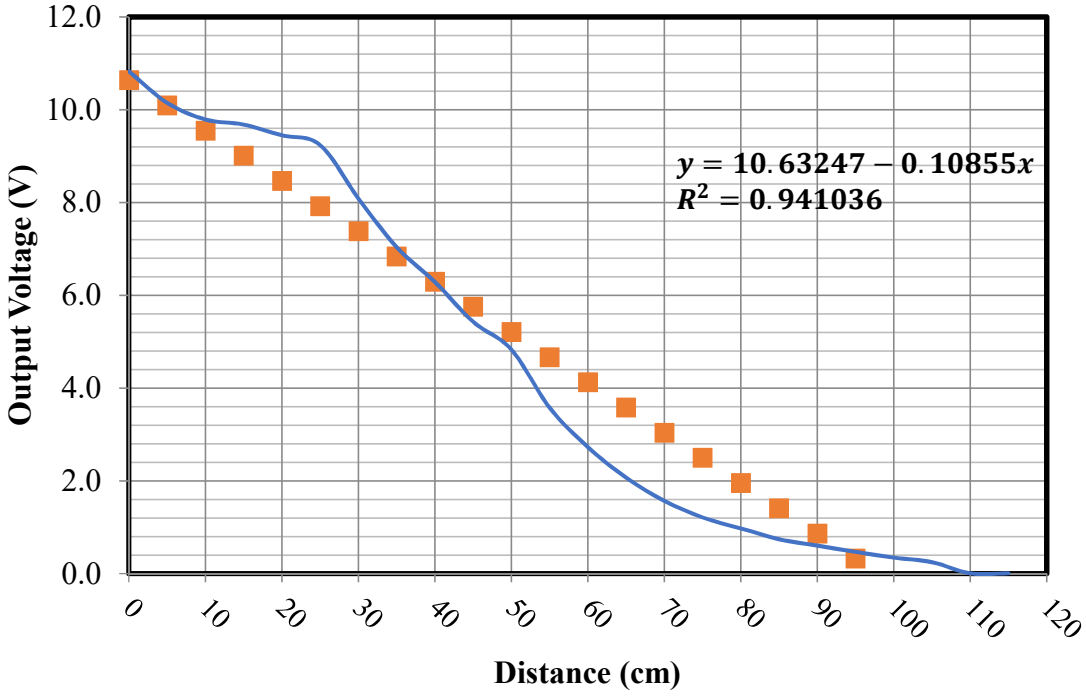

Figure 8.
Relationship between the transfer distance and output voltage of the load loop

The statistic multiple R suggests that efficiency is highly related to the distance between the coils. Moreover, the R-square (R^2) suggests that the distance of the two coils can explain 93.32 percent of the variance in the efficiency tested during the experiment. This result could be in-

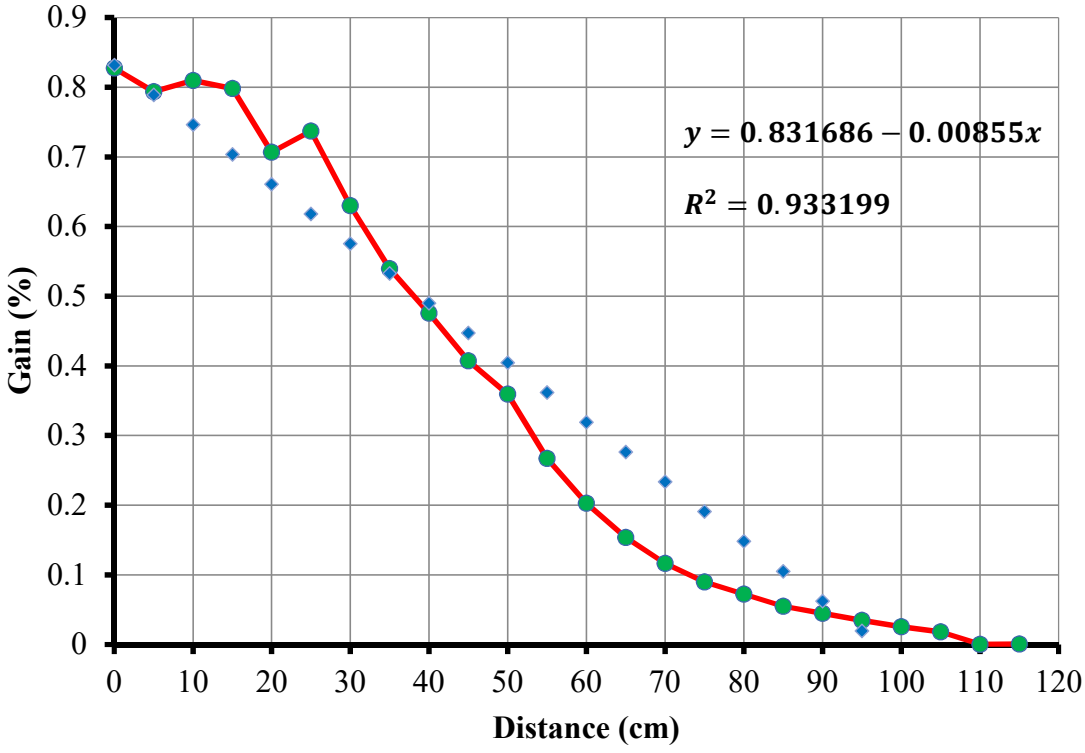

Figure 9.
Relationship between the Voltage Gain and the Separation Distance

Current Integrative Engineering
Volume 2, Issue 1, 42-59, *ISSN: 2995-6307*
DOI: 10.59762/cie5703905421202402051337 44

Distance (cm)	Input			Output		
	Voltage (Volts)	Current (Ampere)	Power (Watts)	Voltage (Volts)	Current (Ampere)	Power (Watts)
0	5.61	7.72	43.3092	8.5	2.05	17.425
5	4.26	8.75	37.275	7.29	1.95	14.2155
10	11.48	2.75	31.57	4.54	1.6	7.264
15	12.63	1.94	24.5022	2.28	1.31	2.9868
20	12.68	1.85	23.458	1.79	0.52	0.9308
25	13.09	1.79	23.4311	1.72	0.31	0.5332
30	13.01	1.75	22.7675	1.702	0.18	0.30636
35	13.29	1.72	22.8588	1.67	0.11	0.1837
40	13.18	1.72	22.6696	1.645	0.07	0.11515
45	13.3	1.69	22.477	1.625	0.04	0.065
50	13.31	1.71	22.7601	1.59	0.02	0.0318
55	13.35	1.69	22.5615	1.5	0.01	0.015

Table 3.
Measured Value for Voltage, Current and Power

terpreted to mean that there is enough evidence to show that the distance between the coils determines the higher gain voltage of the system.

System Efficiency

The power received in the receiver coil divided by the power emitted from the transmitter coil is used to calculate the power transfer efficiency, which describes the direct energy transfer between the transmitter and receiver coils as stated in equation 8. Table 3 and Figure 10 below demonstrate that efficiency increases with decreasing distance. Because of the lower efficiency, there should be more space between the transmitting and receiving coils. The graph also shows that the distance between the two coils has a limit. The graph's intersection with the efficiency zero line occurred at this point. The statistic multiple R suggests that efficiency is highly related to the distance between the coils. Moreover, the R-square (R_2) suggests that 71.15 percent of the variance in the efficiency tested can be explained by the distance of the two coils during the experiment. Moreover, the analysis of variance yielded an F=24.66 which is significant even beyond the 0.01 level. The significance level is 0.000564872. This result could be interpreted to mean that there is enough evidence to show that distance between the coils determines higher efficiency of the prototype. This result finds support from the studies of

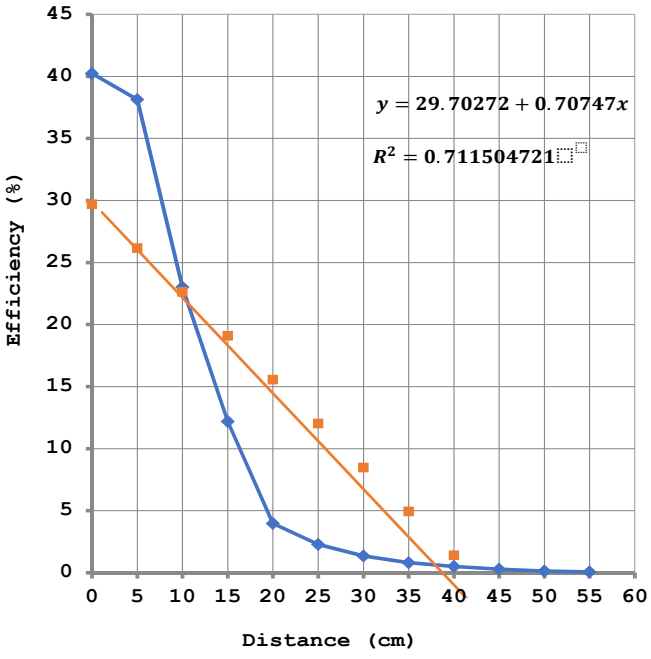

Figure 10.
Relationship between the Transfer Distance and System Efficiency

(Sample et al., 2009), (Kurs et al., 2007), (Park and Kim, 2012) and (Yoon and Ling, 2012).

Voltage Patterns as a Function of Angular Displacements

In this experiment, as shown in Figure 11, the generating coil was maintained in a fixed position while the receiving coil collected samples of the electromagnetic field in and around the generating coil at a fixed distance and with constant angular displacement, completing 360 degrees.

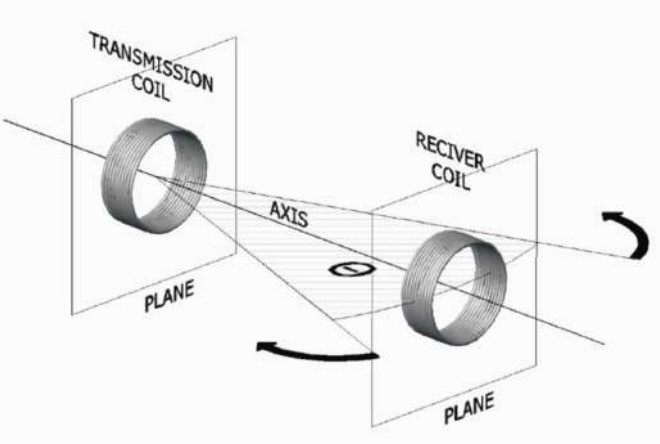

Figure 11.
Experimental Process for the Revolving Coil

The radiation patterns for the producing coil are displayed on the graph in figure 12 below. From this experiment, it can be shown that the energy generated by the producing coil spreads at a 90° angle in front of the coil and at a 90° angle behind the coil. This finding is intriguing since the following experiment will be planned to send the largest amount of forward energy while also taking the rear into consideration for future tests. Additionally, the highest radiation levels are at 345° and 165°, or directly in front and behind the generating coil, respectively (due to the configuration and experiment conditions, the receiving coil had a displacement to the x-axis of around 15°). Given that energy depends on the directivity of the coil, the fact that the pattern is bidirectional has a significant impact on the system's gain calculation. Thus, the radiation pattern's shape will have an impact on efficiency.

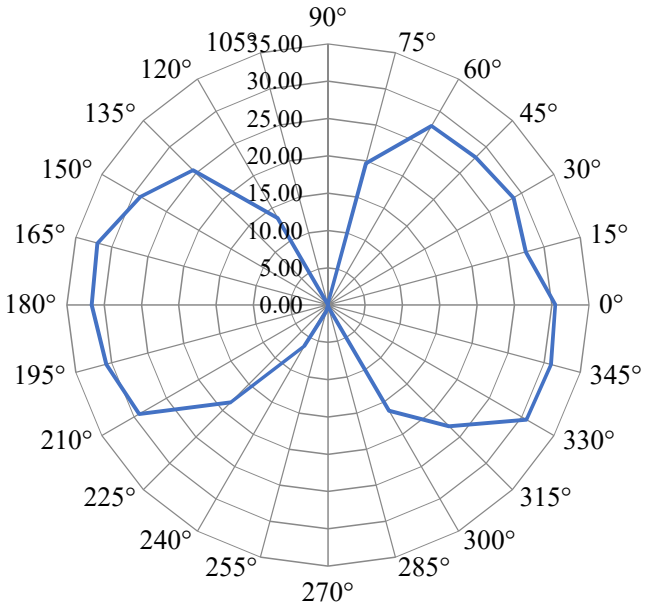

Figure 12.
Voltage Pattern in Different Orientation

To measure the voltage gain both loops were placed facing each other and the receiving loop was moved away at a constant rate from the generating loop. Since the generating loop has constant voltage, the voltage measurement was only performed at the receiving loop for each displacement. The ratio of the voltages was graphed once they had been measured, as seen in figure 14. As seen in the graph, when the two loops are close together, the generating loop sends all its energy to the front, where the receiving loop absorbs it. When the voltage gain is 50%, this is apparent. Considering the wasted radiation rear lobe in Figure 12's radiation pattern, the outcome makes sense. Beyond the 8 cm, as seen in Figure 13. The system's voltage gain is less than 5% at a distance. Using a magnetic field reflecting surface, the back lobe might be recycled.

Testing at Different Frequencies

Figure 14 shows the relationship between the different driving frequencies, the resonant frequency, and the back emf's on the load loop. As depicted on the graph that, driving frequencies have a slight impact on the amplitude side. On the side of resonant frequency, it is seen that there is no effect on the part of driving different frequencies.

Current Integrative Engineering
Volume 2, Issue 1, 42-59, *ISSN: 2995-6307*
DOI: 10.59762/cie5703905421202402051337 44

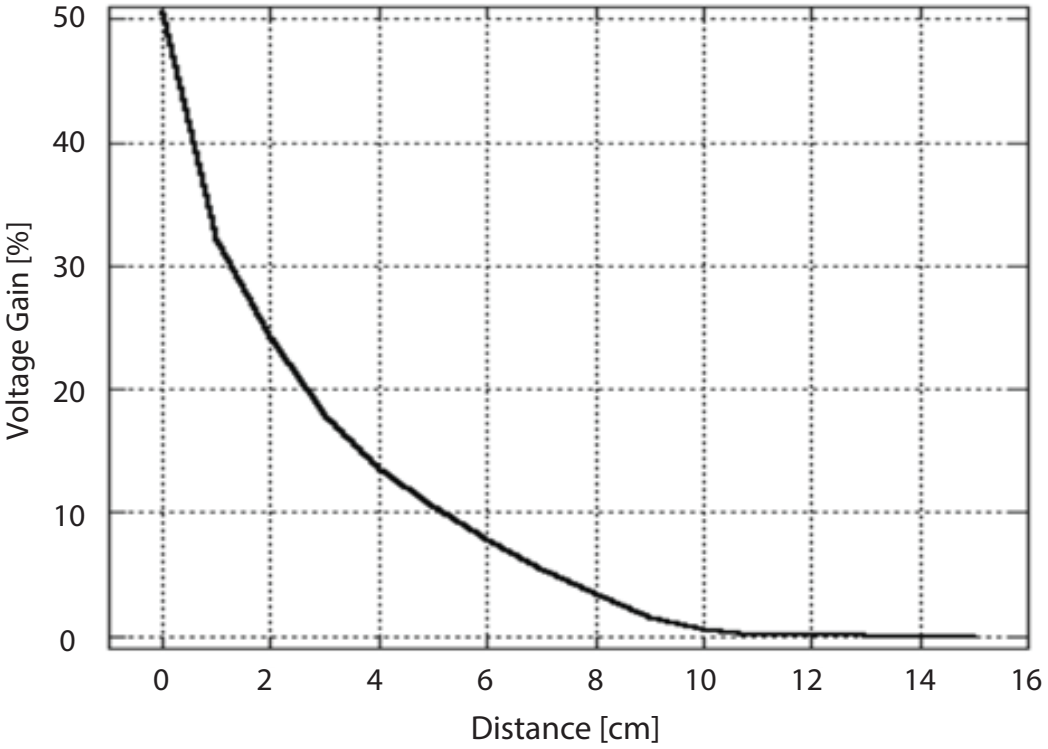

Figure 13.
System's Voltage Gain Relative to Voltage Ratio

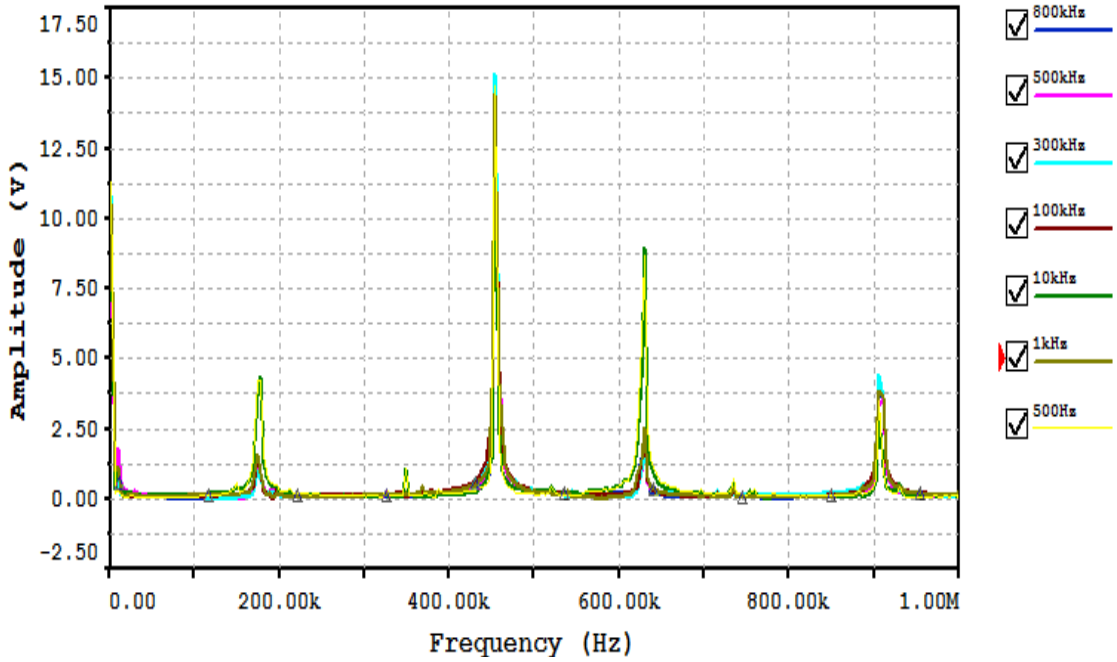

Figure 14.
Relationship Between the Different driving Frequency, Resonant Frequency, and the Output Voltage on Load Loop

Conclusion

Wireless energy transfer has the potential to be improved, and magnetic resonance coupling is the most feasible method in wireless energy transfer. Otherwise, this paper also proved that the electrical energy transmission would transpire the most efficiently in the resonance frequency. The application was used to prove this by using a cell phone, DC motor, LED and bulb. In addition, it can be concluded that the maximum output voltage at the receiver of the resonant wireless energy transfer depends on the size of coil and the input voltage. The transfer of energy could be done effectively by increasing the input voltage. The size and frequency of the device should also be taken into account since the resonance wireless energy transfer device works in the medium- or high-frequency range of electromagnetic fields. The higher the frequency, the closer is the common coil and capacitor to the resonant condition. This work establishes the foundation for creative wireless power technology and presents the potential for the commercial application of cutting-edge electromagnetic resonance based on WPT systems. It has been demonstrated that energy transfer using magnetic coupling resonance technology is entirely practical based on experimental findings and analysis. To obtain the initial and deterministic design parameters of the WPT system comprising resonators and their coupling elements and achieve a pass band at the frequency of interest, straightforward and widely used processes based on electrical circuit theory are applied to the analyses throughout this paper. Additionally, Multisim has been used to simulate circuits. The Power Transfer Efficiency significantly declines as a function of distance outside the coupled mode zone. This demonstrates the hypothesis since the coupled mode resonance phenomena vanishes as the distance between the two antennas grows, and the antennas in the near field operate like conventional transmitting and receiving antennas. It was verified that the distance between the center of the coil plays an important role in the efficiency of the power transfer, decreasing as the center is moved away and reaching its maximum at 0 cm. Besides, the relative angles between the planes of each coil also affect the efficiency, establishing in the experiment that the planes should be placed in a parallel fashion over the same axis. This theoretical model is validated against measured data and shows an excellent average coefficient of determination R2 of 0.937118 which signifies 93.7118 percent of the variation in the distance can be explained through the linear regression relation.

References

Dionigi, M., Costanzo, A. and Mongiardo, M. (2012). Network Methods for Analysis and Design of Resonant Wireless Power Transfer Systems, Wireless Power Transfer - Principles and Engineering Explorations, Dr. Ki Young Kim (Ed.), ISBN: 978-953-307-874-8 https://doi.org/10.5772/25281 PMCid:PMC3332221

Fan, W., Zhang, Y., Ma, H., Zhang, H., & Zhao, Z. (2019). A comprehensive review of wireless power transfer via strongly coupled magnetic resonances. Energies, 12(9), 1740. https://doi.org/10.3390/en12091740

Grajski, K., Tseng, R. and Wheatley, C. (2012). Loosely-Coupled Wireless Power Transfer: Physics, Circuits, Standards. Microwave Workshop Series on Innovative Wireless Power Transmission: Technologies, Systems and Applications (IMWS), 2012, IEEE MTT-S International. https://doi.org/10.1109/IMWS.2012.6215828

Hirayama, H. (2012). Equivalent Circuit and Calculation of Its Parameters of Magnetic Coupled-Resonant Wireless Power Transfer. Wireless Power Transfer - Principles and Engineering Explorations, Dr. Ki Young Kim (Ed.), ISBN: 978-953-307-874-8 https://doi.org/10.5772/28806

Hoang H. and Bien, F. (2012). Maximizing Efficiency of Electromagnetic Res-

onance Wireless Power Transmission Systems with Adaptive Circuits. Wireless Power Transfer-Principles and Engineering Explorations, Dr. Ki Young Kim, ISBN: 978-953-307-874-8 https://doi.org/10.5772/28922

Jang, B.J.,Lee, S. and Yoon, H. (2012). HF-Band Wireless Power Transfer System: Concept, Issues, and Design. Progress In Electromagnetics Research, Vol. 124, page 211-231 https://doi.org/10.2528/PIER11120511

Kim, H.S., Wono, D.H. and Jang, B.J. (2010). Simple design method of wireless power transfer system using 13.56MHz loop antennas. 978-1-4244-6392-3 https://doi.org/10.1109/ISIE.2010.5636910 PMid:19850636

Komaru, T., Koizumi,M., Komurasaki, K., Shibata, T. and Kano, K. (2012).Compact and Tunable Transmitter and Receiver for Magnetic Resonance Power Transmission to Mobile Objects, Wireless Power Transfer - Principles and Engineering Explorations, Dr. Ki Young Kim (Ed.), ISBN: 978-953-307-874-8 https://doi.org/10.5772/28068 PMCid:PMC3304513

Kurs, A., Karalis, A., Moffatt, R., Joannopoulos, J. D., Fisher, P., & Soljačić, M. (2007). Wireless power transfer via strongly coupled magnetic resonances. Science, 317(5834), 83-86. https://doi.org/10.1126/science.1143254 PMid:17556549

Mokalkar, B., Tale, C. and Edle J. (2012). Witricity: A Novel Concept of Power Transfer, International Journal of Engineering Inventions. ISSN: 2278-7461, www.ijeijournal.com Volume 1, Issue 7 (October2012) PP: 51-59

Nnamdi, Ugochukwu & Asianuba, Ifeoma. (2023). Wireless Power Transfer: A Review of Existing Technologies. European Journal of Engineering and Technology Research. 8. 59-66. https://doi.org/10.24018/ejeng.2023.8.3.3038

Niculae, D. M., Stanculescu, M., Deleanu, S., Iordache, M., & Bobaru, L. (2021). Wireless Power Transfer Systems Optimization Using Multiple Magnetic Couplings. Electronics, 10(20), 2463. MDPI AG. https://doi.org/10.3390/electronics10202463

Okasili, I., Elkhateb, A., & Littler, T. (2022). A Review of Wireless Power Transfer Systems for Electric Vehicle Battery Charging with a Focus on Inductive Coupling. Electronics, 11(9), 1355. MDPI AG. https://doi.org/10.3390/electronics11091355

RamRakhyani, A. K., Mirabbasi, S. & Chiao, M. (Feb. 2011). Design and optimization of resonance-based efficient wireless power delivery systems for biomedical implants, IEEE Trans. Biomed. Circuits Syst., vol. 5, no. 1, pp. 48-63 https://doi.org/10.1109/TBCAS.2010.2072782 PMid:23850978

Sample, A. P., Meyer, D. A., & Smith, J. R. (2011). Analysis, experimental results, and range adaptation of magnetically coupled resonators for wireless power transfer. IEEE Transactions on Industrial Electronics, 58(2), 544-554. https://doi.org/10.1109/TIE.2010.2046002

Sedwick, R. (2012). A Fully Analytic Treatment of Resonant Inductive Coupling in the Far Field, Wireless Power Transfer - Principles and Engineering Explorations, Dr. Ki Young Kim (Ed.), ISBN: 978-953- 307-874-8

Sugiyama, H. (2012). Performance Analysis of Magnetic Resonant System Based on Electrical Circuit Theory, Wireless Power Transfer - Principles and Engineering Explorations, Dr. Ki Young Kim (Ed.), ISBN: 978-953-307-874-8 https://doi.org/10.5772/25252

Trezise, T. (2011), Modelling Inductively Coupled Coils for Wireless Implantable Bio Sensors, A Novel Approach Using the Finite Element Method, University of Victoria

Van Mulders J, Delabie D, Lecluyse C, Buyle C, Callebaut G, Van der Perre L, De Strycker L., (2022) Wireless Power Transfer: Systems, Circuits, Standards, and Use Cases. Sensors (Basel). 22(15):5573. https://doi.org/10.3390/s22155573 PMid:35898075 PMCid:PMC9371050

Zhang, Y., Zhao, Z., & Li, S. (2018). A generalized power control algorithm for optimizing efficiency and load sharing in multi-coil wireless power transfer systems. IEEE Transactions on Power Electronics, 33(2), 1507-1523. https://doi.org/10.1109/TPEL.2017.2748161